

Towards quantification of the crucial impact of Auger recombination for the efficiency droop in (AlInGa)N quantum well structures

Anna Nirschl,^{1,2,*} Michael Binder,¹ Marina Schmid,¹ Ines Pietzonka,¹
Hans-Jürgen Lugauer,¹ Roland Zeisel,¹ Matthias Sabathil,¹
Dominique Bougeard,² and Bastian Galler¹

¹OSRAM Opto Semiconductors GmbH, Leibnizstraße 4, 93055 Regensburg, Germany

²Institut für Experimentelle und Angewandte Physik, Universität Regensburg,
Universitätstraße 31, 93040 Regensburg, Germany

*Anna.Nirschl@osram-os.com

Abstract: Recent experimental investigations on the reduction of internal quantum efficiency with increasing current density in (AlInGa)N quantum well structures show that Auger recombination is a significant contributor to the so-called "droop" phenomenon. Using photoluminescence (PL) test structures, we find Auger processes are responsible for at least 15 % of the measured efficiency droop. Furthermore, we confirm that electron-electron-hole (*nnp*) is stronger than electron-hole-hole (*npp*) Auger recombination in standard LEDs. The ratio of respective Auger coefficients is determined to be in the range $1 < C_{nnp}/C_{npp} \leq 12$. This asymmetry is shown to limit the detection efficiency of Auger processes in our PL-based approach.

© 2016 Optical Society of America

OCIS codes: (250.5230) Photoluminescence; (230.3670) Light-emitting diodes; (230.5590) Quantum-well, -wire and -dot devices.

References and links

1. J. Piprek, "Efficiency droop in nitride-based light-emitting diodes," *Phys. Status Solidi A* **207**, 2217 (2010).
2. A. David and M. J. Grundmann, "Droop in InGaN light-emitting diodes: A differential carrier lifetime analysis," *Appl. Phys. Lett.* **96**, 103504 (2010).
3. M. F. Schubert, S. Chhajed, J. K. Kim, E. F. Schubert, D. D. Koleske, M. H. Crawford, S. R. Lee, A. J. Fischer, G. Thaler, and M. A. Banas, "Effect of dislocation density on efficiency droop in GaInN/GaN light-emitting diodes," *Appl. Phys. Lett.* **91**, 231114 (2007).
4. Y. C. Shen, G. O. Mueller, S. Watanabe, N. F. Gardner, A. Munkholm, and M. R. Krames, "Auger recombination in InGaN measured by photoluminescence," *Appl. Phys. Lett.* **91**, 141101 (2007).
5. A. Laubsch, M. Sabathil, J. Baur, M. Peter, and B. Hahn, "High-power and high-efficiency InGaN-based light emitters," *IEEE Trans. Electron. Devices* **57**, 79 (2010).
6. E. Kioupakis, P. Rinke, K. T. Delaney, and C. G. Van de Walle, "Indirect Auger recombination as a cause of efficiency droop in nitride light-emitting diodes," *Appl. Phys. Lett.* **98**, 161107 (2011).
7. A. Hangleiter, F. Hitzel, C. Netzel, D. Fuhrmann, U. Rossow, G. Ade, and P. Hinze, "High excitation carrier density recombination dynamics of InGaN/GaN quantum well structures: possible relevance to efficiency droop," *Phys. Rev. Lett.* **95**, 022106 (2005).
8. J. Iveland, L. Martinelli, J. Peretti, J. S. Speck, and C. Weisbuch, "Direct measurement of Auger electrons emitted from a semiconductor light-emitting diode under electrical injection: identification of the dominant mechanism for efficiency droop," *Phys. Rev. Lett.* **110**, 177406 (2013).
9. M. Binder, A. Nirschl, R. Zeisel, T. Hager, H.-J. Lugauer, M. Sabathil, D. Bougeard, J. Wagner, and B. Galler, "Identification of *nnp* and *npp* Auger recombination as significant contributor to the efficiency droop in (GaIn)N quantum wells by visualization of hot carriers in photoluminescence," *Appl. Phys. Lett.* **103**, 071108 (2013).

10. B. Galler, H.-J. Lugauer, M. Binder, R. Hollweck, Y. Folwill, A. Nirschl, A. Gomez-Iglesias, B. Hahn, J. Wagner, and M. Sabathil, "Experimental determination of the dominant type of Auger recombination in InGaN quantum wells," *Appl. Phys. Express* **6**, 112101 (2013).
11. R. Vaxenburg, A. Rodina, E. Lifshitz, and A. L. Efros, "The role of polarization fields in Auger-induced efficiency droop in nitride-based light-emitting diodes," *Appl. Phys. Lett.* **103**, 221111 (2013).
12. F. Bertazzi, M. Goano, and E. Bellotti, "Numerical analysis of indirect Auger transitions in InGaN," *Appl. Phys. Lett.* **101**, 011111 (2012).
13. A. Hangleiter, D. Fuhrmann, M. Grewe, F. Hitzel, G. Klewer, S. Lahmann, C. Netzel, N. Riedel, and U. Rossow, "Towards understanding the emission efficiency of nitride quantum wells," *Phys. Status Solidi A* **201**, 2808 (2004).
14. A. Nirschl, M. Binder, M. Schmid, M. M. Karow, I. Pietzonka, H.-J. Lugauer, R. Zeisel, M. Sabathil, D. Bougeard, and B. Galler, "Transport and capture properties of auger-generated high-energy carriers in (AlInGa)N quantum well structures," *J. Appl. Phys.* **118**, 033103 (2015).
15. J. Pipek, F. Rammer, and B. Witzigmann, "On the uncertainty of the Auger recombination coefficient extracted from InGaN/GaN light-emitting diode efficiency droop measurements," *Appl. Phys. Lett.* **106**, 101101 (2015).
16. E. Kioupakis, Q. Yan, D. Steiauf, and C. G. Van de Walle, "Temperature and carrier-density dependence of Auger and radiative recombination in nitride optoelectronic devices," *New J. Phys.* **15**, 125006 (2013).
17. J. Hader, J. V. Moloney, B. Pasenow, S. W. Koch, M. Sabathil, N. Linder, and S. Lutgen, "On the importance of radiative and Auger losses in GaN-based quantum wells," *Appl. Phys. Lett.* **92**, 261103 (2008).
18. K. T. Delaney, P. Rinke, and C. G. Van de Walle, "Auger recombination rates in nitrides from first principles," *Appl. Phys. Lett.* **94**, 191109 (2009).
19. B. Galler, P. Drechsel, R. Monnard, P. Rode, P. Stauss, S. Froehlich, W. Bergbauer, M. Binder, M. Sabathil, B. Hahn, and J. Wagner, "Influence of indium content and temperature on Auger-like recombination in InGaN quantum wells grown on (111) silicon substrates," *Appl. Phys. Lett.* **101**, 131111 (2012).
20. D. Schiavon, M. Binder, M. Peter, B. Galler, P. Drechsel, and F. Scholz, "Wavelength-dependent determination of the recombination rate coefficients in single-quantum-well GaInN/GaN light emitting diodes," *Phys. Status Solidi B* **250**, 283 (2012).
21. I. E. Titkov, S. Y. Karpov, A. Yadav, V. L. Zerova, M. Zlonas, B. Galler, M. Strassburg, I. Pietzonka, H.-J. Lugauer, and E. U. Rafailov, "Temperature-dependent internal quantum efficiency of blue high-brightness light-emitting diodes," *IEEE J. Quantum Electron.* **50**, 911 (2014).
22. Y. Ohba and A. Hatano, "A study on strong memory effects for Mg doping in GaN metalorganic chemical vapor deposition," *J. Cryst. Growth* **145**, 214 (1994).
23. U. Kaufmann, M. Kunzer, H. Obloh, M. Maier, C. Manz, A. Ramakrishnan, and B. Santic, "Origin of defect-related photoluminescence bands in doped and nominally undoped GaN," *Phys. Rev. B* **59**, 5561 (1999).
24. S. Nakamura, N. Iwasa, M. Senoh, and T. Mukai, "Hole compensation mechanism of p-type GaN films," *Jpn. J. Appl. Phys.* **31**, 1258 (1992).
25. F. Bertazzi, M. Goano, X. Zhou, M. Calciati, G. Ghione, M. Matsubara, and E. Bellotti, "Auger processes in InGaN/GaN LEDs: full-band modeling and experiments," in *IWN 2014, International Workshop on Nitride Semiconductors, Wroclaw*.

1. Introduction

The reduction of internal quantum efficiency (IQE) at current densities exceeding $1 - 10 \text{ Acm}^{-2}$ in GaN-based light-emitting diodes (LEDs), the so-called "droop" phenomenon, has troubled industry and researchers alike for many years [1, 2]. The most frequently discussed possible origins of this efficiency droop are carrier leakage [3], Auger recombination [4–6] and density activated defect recombination [7]. Only recently, two sophisticated experiments were presented which identify Auger recombination as a significant contributor [8, 9]. In this quantum well (QW) internal loss process, the recombination energy from a band-to-band transition is either transferred to an electron (*mp*-Auger) in the conduction or a hole (*npp*-Auger) in the valence band. In the report by Binder et al. [9], at least 1 % of the droop was ascribed to these processes. The authors deduced that the realistic percentage might be much higher due to fundamental limitations in detection efficiency. In order to optimize LED operation and thus identify the most promising concepts to overcome the high-current losses, it is essential to determine the main contribution to this droop. In this letter, we increase the fraction of droop which can be ascribed to Auger processes to at least 15 % by applying the approach by Binder et al. to optimized test structures. Furthermore, we experimentally confirm that C_{mp} exceeds C_{npp} [10, 11] in contrast to many theoretical calculations [6, 12] and additionally quantify the

ratio to $1 < C_{nnp}/C_{npp} \leq 12$.

2. Method

For all samples discussed in this letter, a 4 μm thick GaN buffer was deposited on a GaN nucleation layer by metal-organic vapor phase epitaxy on a *c*-plane sapphire substrate. The active layers contain one green- and several UV-emitting InGaN QWs with 22 % and 10 % indium content, respectively. The 3 nm thick wells are separated by 7 nm thick $\text{Al}_x\text{Ga}_{1-x}\text{N}$ barriers. A GaN cap layer completes the deposition. More details on the structures are given in the sections 3.2 and 3.3.

A photoluminescence (PL) setup is used to resonantly excite the green-emitting QWs with a 450 nm laser diode at 12 K. By this method carrier densities similar to typical LED operation were achieved; hence a significant reduction in IQE was measured. It has been shown that no carriers are directly created in the UV wells by this optical pumping [9]. The observed UV luminescence is thus a proof of both high-energy electrons and holes generated from Auger processes in the green and transferred to the UV QWs. To determine the fraction of the droop which can be ascribed to Auger recombination detected through PL, the missing green photons, which are lost due to droop, need to be correlated to the detected UV luminescence. We introduce the parameter β which will be explained in the following: A measure for the IQE of the green QWs is obtained by dividing the number of green photons $N_{\text{green}}^{\text{Ph}}$ by the excitation power P . The missing green photons in arbitrary units can be calculated from the IQE reduction with respect to $\left(\frac{N_{\text{green}}^{\text{Ph}}}{P}\right)_{\text{ideal}}$, which corresponds to 100 %. Under the reasonable assumption that SRH recombination is not relevant at 12 K due to defect freeze-out and that no other non-radiative process reduces the IQE in the low-current regime from 100 %, it follows $\left(\frac{N_{\text{green}}^{\text{Ph}}}{P}\right)_{\text{ideal}} = \max\left[\frac{N_{\text{green}}^{\text{Ph}}}{P}\right]_P$ [13]. It has been shown for undoped samples that both the number of lost green photons due to droop and the Auger recombination measured as UV luminescence scale with the cubed carrier density in the green QW for all P [9, 14]. The ratio of these two terms (in arbitrary units) is thus a constant

$$\beta := \frac{\left(\frac{N_{\text{green}}^{\text{Ph}}}{P}\right)_{\text{ideal}} - \frac{N_{\text{green}}^{\text{Ph}}}{P}}{\frac{N_{\text{UV}}^{\text{Ph}}}{P}}, \quad (1)$$

where $N_{\text{UV}}^{\text{Ph}}$ is the number of detected UV photons. This finding proves that Auger recombination, as the cause of the UV luminescence, contributes to the droop.

Assuming that Auger recombination is the only origin of the droop, the lost green photons are caused by the total Auger recombination rate. Since electrons and holes are required for the generation of photons, the smaller of the two densities in the UV wells limits their luminescence. The corresponding generation rates are determined by the Auger recombination rate with coefficient C_{nnp} or C_{npp} multiplied by the respective transfer probability α_n or α_p for high-energy electrons and holes into the UV wells. From these considerations, β_{Auger} gives the constant ratio of Eq. (1) in the case that Auger recombination is the only cause of the droop:

$$\beta_{\text{Auger}} = \frac{C_{nnp} + C_{npp}}{\min[\alpha_n C_{nnp}, \alpha_p C_{npp}]}. \quad (2)$$

Considering that one electron and one hole, and thus two Auger processes, are necessary to generate a single UV photon which can be detected in our experiment, $2/\beta$ represents the minimum detection efficiency of Auger processes contributing to droop [9]. Low values of

the detection efficiency can thus have two reasons: 1) The existence of other processes, which contribute to the droop but do not generate high-energy carriers and thus no UV luminescence for fundamental reasons and 2) Auger processes that are not visualized. As can be seen from Eq. (2), any difference in Auger coefficients decreases the detection efficiency, since not every high-energy carrier finds a recombination partner in the UV QW.

3. Results and Discussion

The straightforward way to reduce the limitation of the detection efficiency with respect to an asymmetry in type of Auger processes is to enhance the lower of the two generation rates of high-energy carriers. Increasing one type of Auger recombination rate more than the other can be realized by introducing background carriers in the green QWs as will be shown by the following evaluations using an extended *ABC* rate equation model [10].

3.1. Role of Background Carriers: Theoretical Considerations

Due to the uncertainty in extracting the *C* recombination coefficient from experimental measurements [15] and ongoing discussions on theoretical models [16], values ranging from $3.5 \times 10^{-34} \text{ cm}^6 \text{ s}^{-1}$ to $1 \times 10^{-29} \text{ cm}^6 \text{ s}^{-1}$ have been reported [2, 4–6, 12, 17–20]. Nevertheless, qualitative trends can be evaluated by using a consistent set of parameters, e.g. from IQE fits at room temperature of a SQW emitting at 540 nm [20]. To account qualitatively for the cryogenic temperature we increase the SRH recombination lifetimes by a factor of 100 whereas the *B* and *C* coefficients were not changed due to discordant temperature trends found in literature [19, 21]: $\tau_n = 100 \times 5 \times 10^{-6} \text{ s}$, $\tau_p = 100 \times 5 \times 10^{-6} \text{ s}$, $B = 1 \times 10^{-12} \text{ cm}^3 \text{ s}^{-1}$, $C_{nnp} + C_{ppp} = 1 \times 10^{-31} \text{ cm}^6 \text{ s}^{-1}$. Since it has been previously suggested by our group that C_{nnp} exceeds C_{ppp} [10], we assume $C_{nnp}/C_{ppp} = 10$ for this evaluation. The resulting influence of different types of background carriers on the calculated IQE as a function of excitation carrier density *x* is shown in Figs. 1(a) and 1(b). In all cases, the IQE is reduced (even in the low excitation regime) due to the increased total Auger recombination rate resulting from the added background carrier density. This effect is more pronounced when increasing the electron background density since C_{nnp} was assumed to be larger than C_{ppp} . With increasing excitation density, the impact of the background carrier density on the total carrier density (sum of background and excitation carrier density) becomes less and less pronounced so that the IQEs in Fig. 1(a) and 1(b) approach each other.

In the next step, we calculate β_{Auger} for test structures containing UV- and green-emitting QWs featuring different background carrier types, leading to Figs. 1(c) and 1(d). Considering added background electrons, the enhancement of the already stronger *nnp*-Auger recombination rate due to our assumption of $C_{nnp} > C_{ppp}$ leads to even more electrons which do not have a recombination partner in the UV wells and thus cannot be detected as luminescence. Increasing the optical excitation density reduces the impact of the background carriers on the ratio of Auger recombination rates and thus on the detection efficiency. Hence, a dependence of β on excitation carrier density *x* is expected. In contrast to the constant value of β_{Auger} in undoped samples, Eq. (2) predicts a parameter β_{Auger, n_0} for added background electrons n_0 , expressed as

$$\beta_{Auger, n_0} = \frac{C_{nnp} \frac{(x+n_0)}{x} + C_{ppp}}{\alpha_p C_{nnp}} > \beta_{Auger} \text{ (undoped)} \quad (3)$$

assuming that holes limit the UV luminescence in the undoped case, i.e. $\frac{C_{nnp}}{C_{ppp}} > \frac{\alpha_p}{\alpha_n}$ [14]. Similar considerations for added background holes p_0 define an excitation carrier density dependent

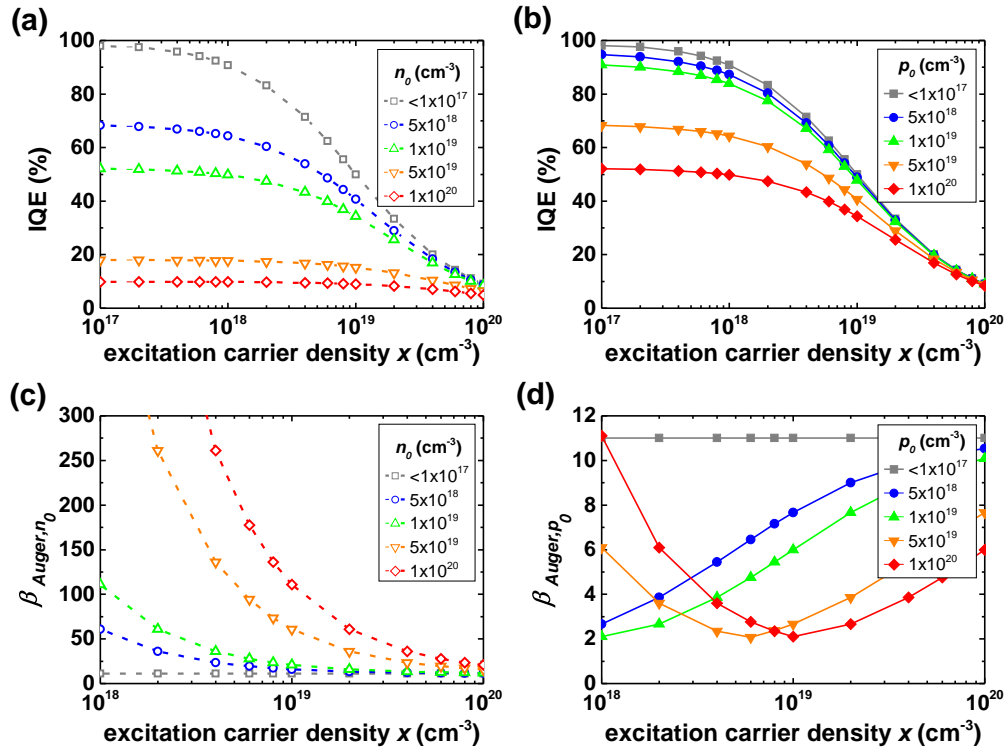


Fig. 1. Calculated IQE as a function of excitation carrier density for different background (a) electron and (b) hole densities assuming $C_{nnp} = 10 \times C_{npp}$. The β_{Auger, n_0} and β_{Auger, p_0} values calculated from Eqs. (3) and (4) assuming $\alpha_n = \alpha_p = 1$ are shown in (c) and (d), respectively.

parameter β_{Auger, p_0} :

$$\beta_{Auger, p_0} = \frac{C_{nnp} \frac{x}{(x+p_0)} + C_{npp}}{\min[\alpha_n C_{nnp} \frac{x}{(x+p_0)}, \alpha_p C_{npp}]}. \quad (4)$$

The qualitative trends for different background electron and hole densities under the assumption $\alpha_n = \alpha_p = 1$ are shown in Figs. 1(c) and 1(d), respectively. For added background electrons, all β_{Auger, n_0} values are higher than the constant $\beta_{Auger, n_0=0} = \beta_{Auger, p_0=0} = \beta_{Auger} = 11$ expected for the undoped sample. This value only depends on the asymmetry in type of Auger recombination rate which we have assumed in the considered case. The increasing β_{Auger, n_0} values with increasing n_0 can be explained by the rising ratio in nnp - to npp -Auger recombination rates and thus an increasing density of electrons which lack holes for the radiative recombination in the UV QWs. At high excitation carrier densities, all β_{Auger, n_0} asymptotically approach the constant value of the undoped sample. This monotonic behavior can be explained by the decreasing influence of background electrons on the total carrier density and thus on the Auger recombination rates.

In Fig. 1(d), added background holes lead to β_{Auger, p_0} values lower than the constant $\beta_{Auger} = 11$ for all excitation carrier densities shown. This can be explained by the reduced asymmetry in type of Auger recombination rates. For the highest densities of background holes, we do not observe a monotonic behavior of β_{Auger, p_0} with increasing excitation carrier density. At low excitation carrier densities, the enhancement of the npp -Auger recombination rate due

to the increased p_0 overcompensates the lower Auger coefficient C_{npp} in the ratio of the Auger recombination rates so that holes limit the UV emission. At the turning point where both processes generate the same density of high-energy carriers in the UV wells, the minimum value of β will be achieved which thus only depends on the transfer probabilities. It has the smallest possible value of 2 in the considered case, which assumes 100 % transfer probability of electrons and holes into the UV wells. Further increasing the excitation carrier density then leads to electrons limiting the detection efficiency. Hence, the experimental implementation of these considerations can clarify which type of Auger recombination dominates the droop.

3.2. Experimental Approach

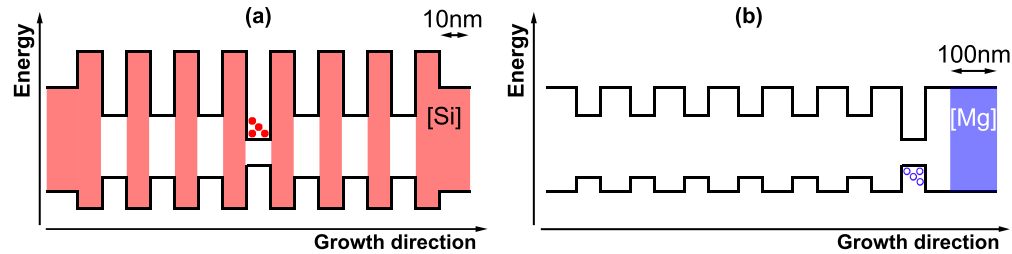


Fig. 2. Schematic illustration of the bandstructure and the doping of layers in the (a) Si series and (b) Mg series.

For this purpose, two different sample series were grown. The Si (*n*-type) series contains three UV QWs both below and above a single green QW. The buffer, all barriers and the cap layer are doped with a constant silicon concentration as illustrated in Fig. 2(a). We varied this level from 0 to $1 \times 10^{19} \text{ cm}^{-3}$ for the four wafers of this series. For the Mg (*p*-type) series, six UV QWs were grown below a single green QW and separated by GaN barriers. Due to the memory effect of the precursor Cp_2Mg [22], only a 100 nm thick GaN cap on top of the layer stack is doped with a constant magnesium concentration (see Fig. 2(b)). This keeps the capture wells at good quality and thus free of doping-related defect recombination [23]. We chose the constant doping concentration between 0 and $8 \times 10^{19} \text{ cm}^{-3}$ for the three wafers of the Mg series. We verified that in both series the introduced doping changes the background carriers in the green but not in the higher-energetic UV QWs from the experimental PL wavelengths and from Schrödinger-Poisson simulations. Both show a blue-shift from about 550 nm to 535 nm in the low excitation regime at RT due to the screening of the QCSE in the green QW. The peak wavelength of the UV QW is rather constant at about 400 nm for all samples. Considering that Mg is known to have a much lower doping efficiency than Si [24], the maximum doping concentrations for both types were chosen such that the background carrier densities introduced into the green QWs are comparable [10]. We note that a dopant freeze-out in the sense of a reduced free carrier density in the QWs is not expected since the energetically most favorable states are located in the QWs and not at the donor/acceptor sites as they are in a bulk material.

Using temperature dependent PL measurements, we checked that all QWs still do not show significant SRH-defect recombination. For the undoped reference samples of both series, a constant factor between the number of UV photons and the Auger rate in the green QWs determined by $(N_{green}^{Ph})^{3/2}$ was obtained, proving that Auger recombination and not direct filling of the QWs is the reason for the observed UV luminescence even when using GaN barriers. Although the asymmetric Mg-doping leads to a potential drop across the whole epitaxial stack, Schrödinger-Poisson simulations revealed almost no change in microscopic electric field of the UV QWs and separating barriers. This suggests no difference in transfer probabilities of high-

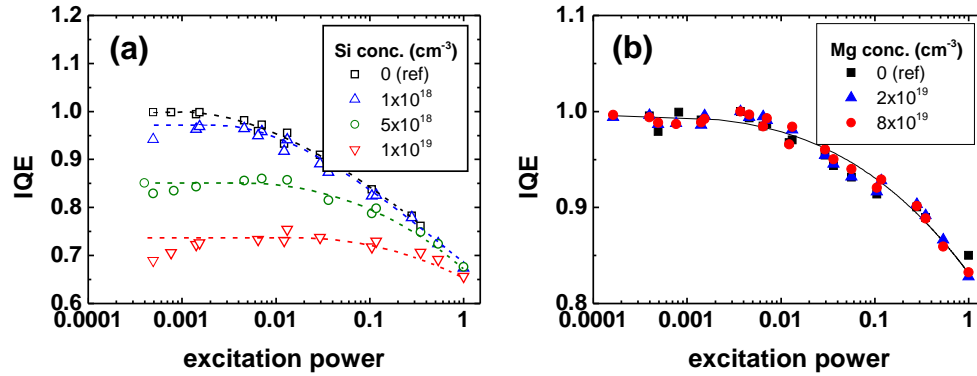


Fig. 3. Normalized low temperature PL IQE of samples featuring different (a) Si and (b) Mg concentrations. The maximum of the former has been chosen such that the high excitation values are comparable as to be expected from theory. Lines are guides to the eye.

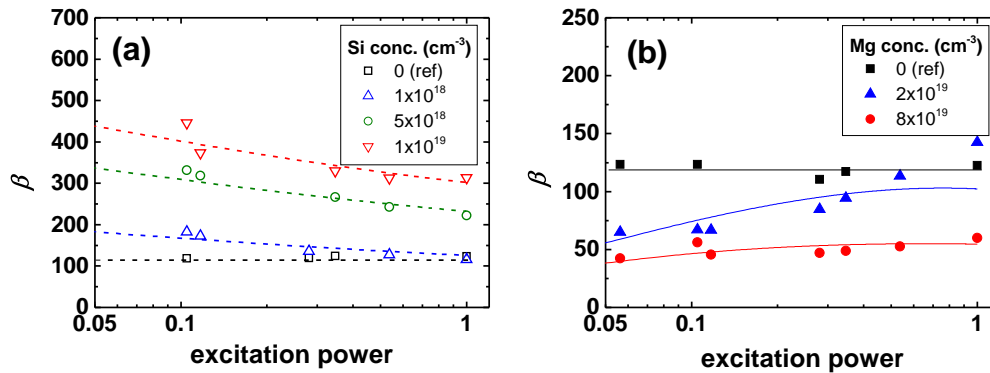


Fig. 4. β determined from Eq. (1) as a function of the excitation power of the (a) Si and (b) Mg series. Lines are guides to the eye.

energy carriers due to hot carrier transport effects. Hence, we interpret all changes in β as a result from a change in the ratio of *nnp*- to *npp*-Auger recombination rate in the green QWs.

Going back to Fig. 1(a), the extended *ABC* rate equation model suggests lower IQE values over the whole excitation regime for increasing *n*-type doping concentrations due to the enhanced Auger recombination rate. Hence, the IQE in the low excitation regime is no longer 100 % but reduced by a factor γ compared to the intrinsic case. The experimental data from the Si series suggest that this is indeed the case: Firstly, we observed the measured intensity of the green emission to be strongly reduced with increasing doping concentration (not shown). Secondly, a normalization of the low excitation IQE to 100 % would lead to increasing values at high excitations for increasing doping concentrations (compare the reduced drop from the maximum IQE with increasing doping concentration in Fig. 3(a) in contrast to the theory described in section 3.1. Hence, we normalized the IQE such that the high excitation efficiency is comparable for all samples in Fig. 3(a). As can be seen from the calculated trend of the IQE in Fig. 1(a) where the curves show no intersection, this is the minimum correction necessary to account for the enhanced Auger recombination. For the Mg series in Fig. 3(b), the maximum IQE of all samples was normalized to 100 %. In this case, we can exclude a strong reduction in IQE due to the enhanced Auger recombination rate because the experimental IQE trend for

all doping concentrations is the same, as predicted for a low C_{npp} in Fig. 1(b). Consequently, although the maximum background carrier concentrations were chosen to be similar in both series, we observe a stronger reduction of the IQE in the Si than in the Mg series. From this experimental result, which is independent of any model assumptions, we conclude that the total Auger recombination rate is even more enhanced by adding background electrons. This suggests that $C_{mp} > C_{npp}$ and that the mnp - dominates over the npp -Auger recombination rate in undoped samples. This finding is in agreement with the experimental observation published by Galler et al. [10].

Next, β for all samples was calculated from Eq. (1) and plotted in Figs. 4(a) and 4(b) as a function of excitation power. Note that the ideal IQE for the Si series is calculated by $\left(\frac{N_{green}^{Ph}}{P}\right)_{ideal} = y \times \max_P \left[\frac{N_{green}^{Ph}}{P}\right]$. In both series, the value of the undoped reference is constant although slightly different due to epitaxial design variations and thus different transfer probabilities of high-energy carriers into the UV QWs. The β for all doped samples approach these values towards higher excitation powers. This is in agreement with the theoretical predictions in Figs. 1(c) and 1(d) which can be explained by the decreasing influence of the background carriers on the Auger recombination rates with increasing excitation carrier density. In the Si series, all β values are higher than the constant reference. Yet, they might still be underestimated owing to the chosen way of scaling down the IQE only by the minimum amount necessary. In the case of Mg, all β are lower than the constant value of the undoped sample. This can be explained by the asymmetry in type of Auger recombination rate which has been reduced due to added background holes; the detection efficiency has thus been increased. The turning point, predicted in Fig. 1(d) and expected at a hole concentration which exactly compensates the smaller generation rate of carriers in the UV wells so that $C_{npp}\alpha_p(p_0 + x) = C_{mp}\alpha_n x$, could not be reached within the experimentally accessible range in background carrier density and excitation power. Note also that the smallest β values, predicted by theory to be obtained at small excitation power, cannot be trusted due to the very low signal to noise ratio (thus not shown in Figs. 4(a) and 4(b)). Therefore, the minimum accessible β in this system could not be determined and the optimum detection efficiency independent of any asymmetry in Auger coefficients could not be verified in this experiment. Nevertheless, the clearly opposite trends for n - and p -type background carriers in the green QWs confirm that mnp - exceeds npp -Auger recombination in InGaN-QWs without high background carrier densities.

3.3. Increase of Detection Efficiency

To obtain further improvement in detection efficiency, we now discuss another approach based on the same idea of decreasing the asymmetry in Auger coefficients. It has been suggested that the interface of the QW plays a significant role in the strength of the Auger recombination [11]. Furthermore, Bertazzi et al. calculated an increasing asymmetry in type of Auger recombination with higher interface polarization charges [25]. This concept motivates the investigation described in the following, where the influence of the barrier material separating the green and UV QWs is analyzed. Two sets of undoped samples were grown, containing either two or five UV QWs both below and above a single green QW. For the four wafers in each set, the aluminum content of the barriers was varied from 50 % to 0 % while keeping the thickness constant (see Fig. 5). This shifts the peak wavelength of the green QW from 560 nm to 510 nm in the low excitation regime at RT due to the reduced QCSE with decreasing Al content. The peak wavelength of the UV QWs stays constant at about 400 nm, since the QCSE has almost no impact in QWs with low In content. A reduced β would be expected from theory, as the interface polarization charges decrease for lower Al content. First, it was checked by temperature dependent excitation with a HeCd-laser emitting at 325 nm that the intensities of both QW

emissions stay constant up to 50 K and thus that the wells have 100 % IQE for low excitation at 12 K.

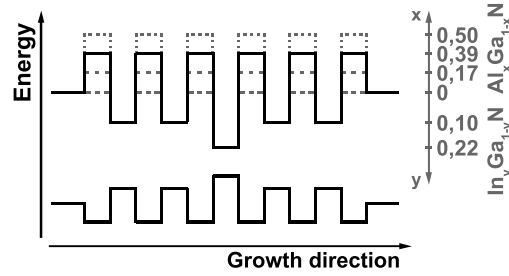


Fig. 5. Schematic illustration of the barrier material series for two UV QWs on each side of the green QW. The influence of the aluminum content on the barrier height is sketched for the conduction band.

In Fig. 6 are shown the results of the experimentally determined β values. Increasing the number of UV QWs from two to five increases the detection of high-energy carriers for a given barrier composition in agreement with our previous result of a higher transfer probability of high-energy carriers [14]. Furthermore, a strong decrease of β is observed when reducing the aluminum content. As we obtain a direct proportionality between the number of UV photons and the Auger recombination rate in the green QWs determined by $(N_{green}^{Ph})^{3/2}$, we verify that once again the droop current (and not direct excitation) causes the observed UV luminescence. Although the energy of the Auger-generated carriers is far above the band-edge of all investigated barrier heights, the transport or relaxation of these high-energy electrons and holes might also be influenced by the change in bandstructure of the quasi-continuum and bound states. Hence, further evaluation would be necessary to discriminate between the reduced asymmetry and the possible change in transfer probability. Nevertheless, by using GaN barriers and five capture wells on each side of the green QW at least $2/13 \approx 15\%$ of the droop can be ascribed to Auger recombination assuming that exactly one *nnp*- and one *npp*-Auger process are necessary to create one UV photon. Under the more reasonable assumption that Auger recombination is the only origin of droop but not all processes can be visualized, it follows from Eq. (2)

$$0.15 < \alpha_p \leq 1 \text{ and } 1 < C_{nnp}/C_{npp} \leq 12. \quad (5)$$

4. Conclusion

In conclusion, we analyzed the influence of added background carriers in the green QWs and thus the ratio of Auger recombination rates on the detection efficiency of these processes in our PL based approach. Adding background holes enhanced the *npp*-Auger recombination rate and thus the generation of high-energy holes. This experiment showed an improved detection efficiency compared to the undoped case. The density of electron-hole-pairs in the UV wells per total Auger recombination rate has thus been increased. The *npp*- falls below the *nnp*-Auger recombination rate in undoped samples, which is in agreement with the results previously reported by our group based on a different experiment [10]. Moreover, we found that $1 < C_{nnp}/C_{npp} \leq 12$. The experimentally observed asymmetry adds to the reduction in detection efficiency due to limitations in transfer probability [14] of high-energy carriers into the detection well. Hence, significantly more than two Auger processes are necessary to create one UV photon in the experiment, which leads to an underestimation of the contribution of Auger processes to droop. Furthermore, we increased the degree of droop that can be assigned to Auger

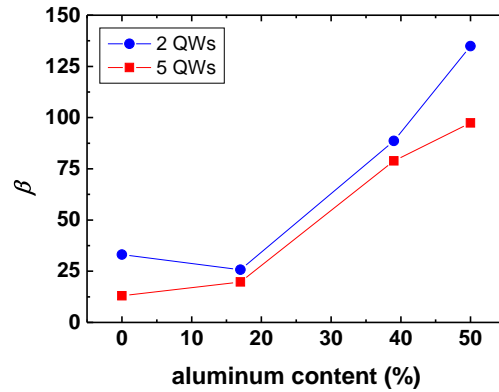


Fig. 6. Influence of barrier material on β for two different numbers of UV QWs on each side of a single green QW.

processes from the previous value of at least 1 % [9] to a minimum of 15 % by reducing the Al content in the barriers separating the generating and capture well of Auger carriers. These results suggest an even higher detection efficiency can be obtained by combining the samples with reduced Al content in the barriers with an enhanced background hole density.

Acknowledgment

We gratefully acknowledge the financial support of the European Union FP7, NEWLED project, grant number 318388.